NASA/TM-1998-208739

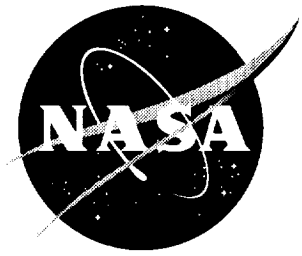

Thermal Output of WK-Type Strain Gauges on Various Materials at Cryogenic and Elevated Temperatures

Matthew K. Kowalkowski, H. Kevin Rivers and Russell W. Smith
Langley Research Center, Hampton, Virginia

National Aeronautics and
Space Administration

Langley Research Center
Hampton, Virginia 23681-2199

October 1998

The use of trademarks or names of manufacturers in the report is for accurate reporting and does not constitute an official endorsement, either expressed or implied, of such products or manufacturers by the National Aeronautics and Space Administration.

Available from:

NASA Center for AeroSpace Information (CASI)
7121 Standard Drive
Hanover, MD 21076-1320
(301) 621-0390

National Technical Information Service (NTIS)
5285 Port Royal Road
Springfield, VA 22161-2171
(703) 605-6000

Abstract

Strain gage thermal output (apparent strain) is one of the largest sources of error associated with the measurement of strain when temperatures vary. In this paper, thermal output of WK-type strain gages is experimentally determined for temperatures ranging from -450°F to 230°F. The gages are installed on both metal specimens and composite laminates of various lay-ups and resin systems. Metal specimens tested include: aluminum-lithium alloy (Al-Li 2195-T87), aluminum alloy (Al 2219-T87), and titanium alloy. Composite materials tested include: graphite toughened-epoxy (IM7/977-2), graphite-bismaleimide (IM7/5260), and graphite-thermoplastic (IM7/K3B). For the composite materials thermal output in both the 0° fiber direction and the 90° fiber direction is measured. The experimentally determined thermal output data are curve fit with a fourth-order polynomial for each of the materials studied. The thermal output data and the polynomials that are fit to the data are compared with those produced by the strain gage manufacturer, and the results and comparisons are presented. Unacceptably high errors in the manufacturer's data are observed at temperatures below -270°F.

Background

The X-33 (see Figure 1) is a half scale Reusable Launch Vehicle (RLV) prototype rocket, based on the Single Stage to Orbit (SSTO) concept, whose project goal is to provide industry with a cost effective vehicle for the next generation of space flight [1]. The success and reusability of future launch systems depend heavily on the reusability of the cryogenic fuel tanks. Space Shuttle (a current space transportation system) cryogenic tanks are designed for only one flight that lasts approximately eight minutes, making the launch process costly and wasteful.

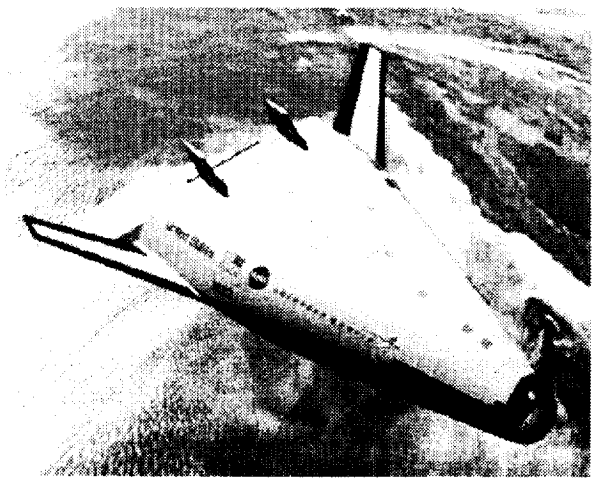

Figure 1. X-33 vehicle.

In order to build a viable RLV, a reusable cryogenic fuel tank must be produced, and the validation of the durability of this cryogenic tank system, which includes the cryogenic insulation, tank structure, and adhesives, requires testing at cryogenic temperatures. This requirement has prompted the NASA Langley Research Center (LaRC) to develop cryogenic thermal-mechanical tests capable of simulating the flight-cycle thermal and mechanical loads for various cryogenic tank concepts. In some of these tests, a series of 1-ft. by 2-ft. rectangular panels are tested to determine their durability while subjected to the thermal and mechanical loads experienced by a tank during flight [2].

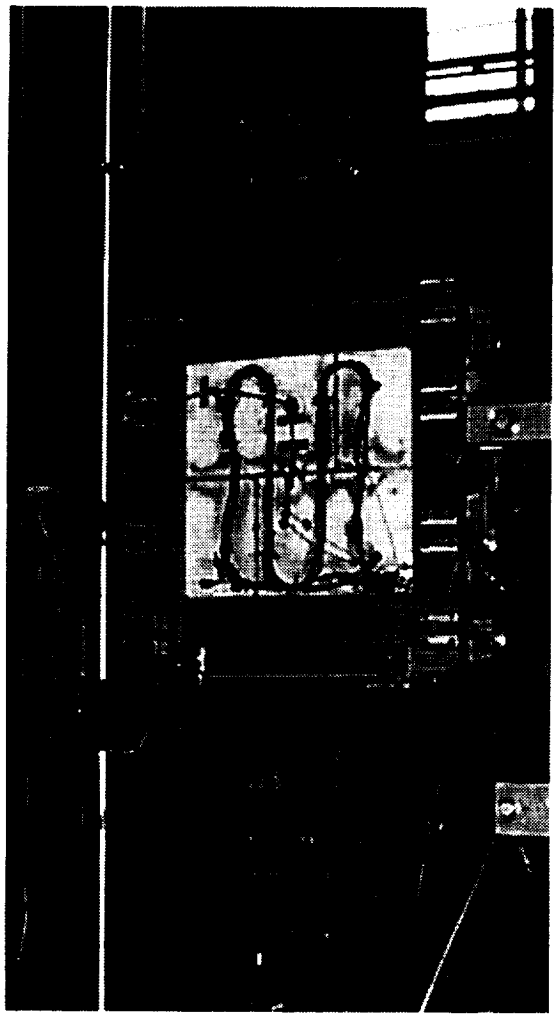

Figure 2. 1-Foot by 2-Foot panel placed in the hydraulic load machine.

The cryogenic thermal-mechanical tests developed at LaRC involve either a metallic or composite sandwich structure (where the sandwich core also serves as a cryogenic insulation) or a metallic or composite stiffened panel (with external cryogenic insulation). Figures 2 and 3 are photographs of the front and back views of one such test. Accurate measurements of strain at temperatures ranging from -423°F to 230°F are required during the tests. Because the electrical resistance of a strain gage varies with both temperature and load, an accurate correction of temperature-induced thermal output is critical for determining the true mechanical strain from strain gage measurements.

Nomenclature

α = the coefficient of thermal expansion of the test material.

α_g = the coefficient of thermal expansion of the strain gage grid.

α_R = coefficient of thermal expansion of the reference material used to compute the manufacturer's curves.

ΔT = the temperature change from the reference temperature.

$(\Delta R/R_0)_{T/O}$ = the relative resistance change from the reference resistance.

β_G = the thermal coefficient of resistance of the gage.

F_G = the gage factor of the gage.

K_t = the transverse sensitivity of the strain gage.

ν_0 = Poisson's ratio of the standard test material used in calibrating the gage for its gage factor.

$e_{T/O}$ = the thermal output (apparent strain) in strain units. The magnitude of strain measured when the gage (mounted to a test material) is subjected to a temperature change.

e_1 = strain magnitude corrected for both thermal output and gage factor variation.

e_2 = indicated or measured strain.

$e_{T/O}\ T_1)$ = thermal output at test temperature T_1.

F^* = gage factor setting used while strain measurement is made.

$F(T_1)$ = gage factor at test temperature.

σ = the stress in the test material.

E = Young's modulus of the test material.

e_P = the thermal output predicted for a strain gage attached to a test material.

e_R = the thermal output for a reference material used to compute the manufacturer's curves.

$e_{T/O}$ = experimentally determined thermal output in microstrain.

T = temperature in °F.

Strain Gage Thermal Output (Apparent Strain)

Temperature-induced thermal output (also called apparent strain) is caused by two algebraically additive components. The first component is the change in electrical resistivity of the gage due to temperature change. This resistance change is independent of any mechanically induced strain on the object to which the gage is bonded. The second component of thermal output is the change in electrical resistivity of the gage due to mechanical strain produced by the difference in coefficients of thermal expansion of the gage material and the material to which the gage is mounted (and in which we want to measure strain).

The cause of the second component is the $\alpha\Delta T$ or "free" thermal expansion of the material to which the gage is bonded. The change in temperature (ΔT) causes an expansion or contraction of the specimen. Because the strain gage is strongly attached to the surface of the material and has a low stiffness, the gage is forced to undergo the same expansion or contraction as the material. This strain of the gage will be registered by an indicator as strain of the specimen, even if no mechanical strain is induced in the specimen. Thus, in order to get an accurate reading of the mechanical strain being placed on the specimen in an environment in which the temperature is changing, it is essential to correct for thermal output due to changes in temperature.

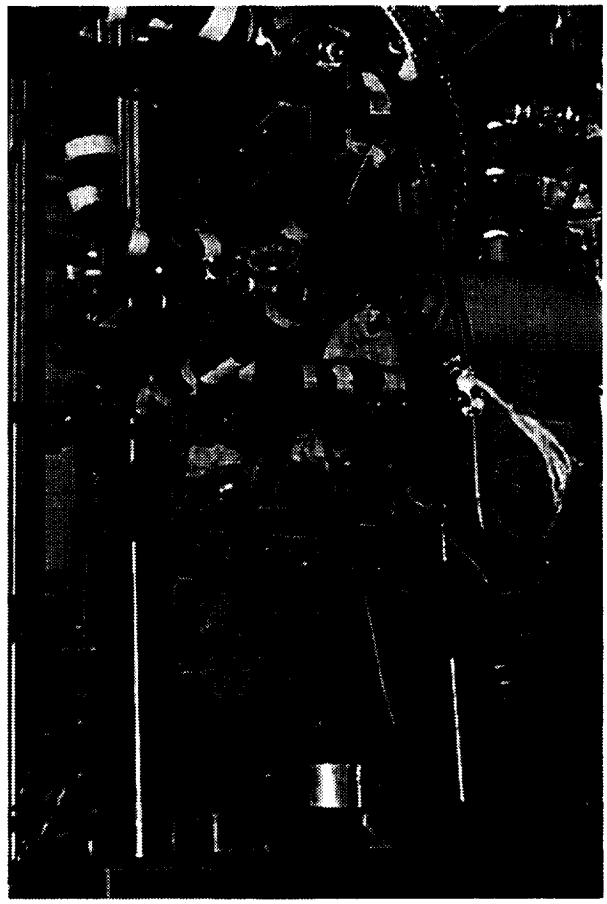

Figure 3. Hydraulic load machine and cryogenic chambers.

Further information about thermal output can be found in reference [3], where equation (1a) is derived. This equation shows how thermal output is the algebraic sum of both components in that the relative change in resistance of the gage is given as:

$$\left(\frac{\Delta R}{R_0}\right)_{T/O} = \left[\beta_G + F_G\left(\frac{1+K_t}{1-\nu_0 K_t}\right)(\alpha - \alpha_G)\right]\Delta T \quad (1a)$$

The thermal output is proportional to the relative resistance change as indicated in the following equation:

$$e_{T/O} = \frac{\left(\frac{\Delta R}{R_0}\right)_{T/O}}{F_G} \quad (1b)$$

One method of experimentally determining thermal output is to take small material specimens (having homogeneous properties), gage them in exactly the same fashion as the test specimen (which locally has the same properties) and then subject these specimens to only thermal loads. Raw strain data collected from this thermal loading of the small specimens can then be utilized to generate thermal output data and the polynomial equations describing those data. These polynomial equations can then be used to determine the true mechanical strain to induce in the test specimen and correct the measured strain data.

In experiments where test specimens are subjected to thermal loads, measured strain data must be corrected for both thermal output and gage factor variations with temperature [3]. The thermal output is dependent on the test specimen material and must be determined experimentally. The gage factor varies linearly with temperature and is not dependent on the test specimen material so data provided by the gage manufacturer is used. Provided that the gage factor and thermal output at temperature are known for the material being tested, Equation 2 below can be used to correct the strain measurement for both thermal output and gage factor variations with temperature.

$$e_1 = [e_2 - e_{T/O}(T_1)]\left(\frac{F^*}{F(T_1)}\right) \qquad (2a)$$

The total strain is a combination of the mechanical strain and the thermal strain and is as follows:

$$e = e_1 + \alpha\Delta T \qquad (2b)$$

For uniaxial loads, the mechanical strain is:

$$e_1 = \frac{\sigma}{E} \qquad (2c)$$

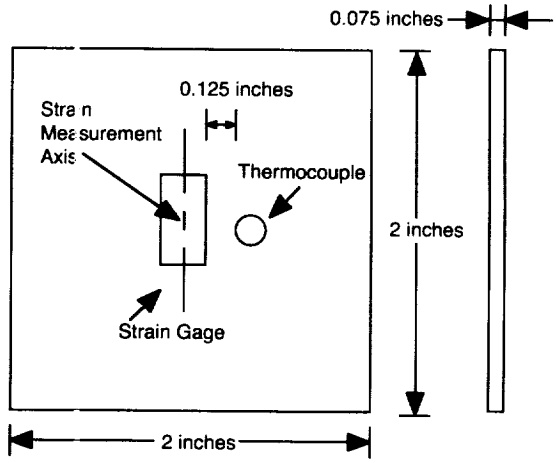

Figure 4. Specimen layout, (dimensions are approximate).

Test Specimens

For this study, values of thermal output were measured for specimens of seven different materials at temperatures ranging from approximately -423 °F to 230 °F. Those specimens include both composite and metallic materials. The specimens were all instrumented with one strain gage mounted in the center of each specimen and one Type-T thermocouple placed to one side of the strain gage as shown in Figure 4. All composite specimens were gaged with WK-00-250BG-350 strain gages, which have a gage factor of 2.02 at 75°F. Three specimens of each material had strain gages oriented along the

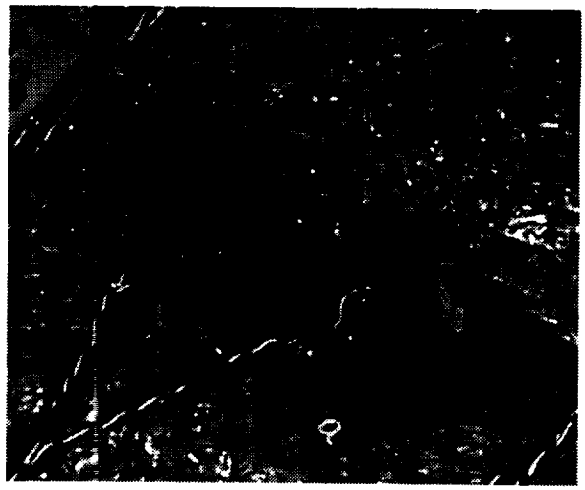

Figure 5. Graphite-K3B co-cured specimens.

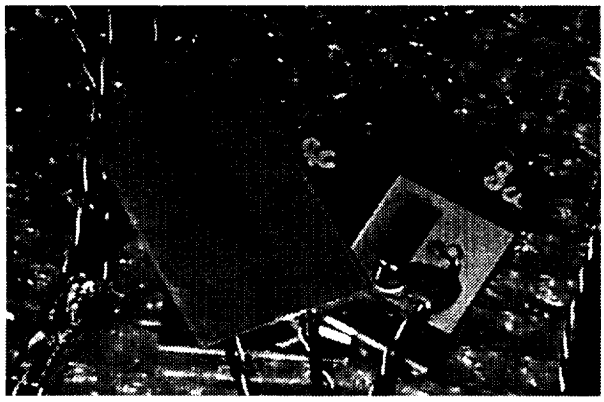

Figure 6. Aluminum-lithium (Al-Li 2195-T87) specimens.

0° fiber direction, and the other three specimens of each material had strain gages oriented along the 90° fiber direction. This was done because composite materials have different coefficients of thermal expansion in orthogonal directions.

The aluminum alloy (Al 2219-T87) and the aluminum lithium (Al-Li 2195-T87) specimens were gaged with WK-13-250BG-350 strain gages which have a gage factor of 2.08 at 75°F, and the titanium alloy specimens were gaged with WK-06-250BG-350 gages which have a gage factor of 2.02 at 75°F. The strain gages were applied using standard installation methods [5].

Six IM7/977-2 graphite toughened-epoxy (GR/EP) and six IM7/5260 graphite-bismaleimide (GR/BMI) specimens were tested. The lay-up of the GR/EP and the GR/BMI specimens was $[\pm 45/0/90/0]_S$ for all twelve of the specimens.

A total of twelve IM7/K3B graphite-thermoplastic (GR/K3B) specimens (see Figure 5) were tested, six of which had a $[0/60/90/-60/0]_S$ lay-up and originated from a facesheet of a co-cured titanium honeycomb sandwich panel which had previously been tested within its elastic limit. The other six specimens were fabricated from a cured laminate with a $[0/45/90/-45]_S$ lay-up. Three of each of the co-cured and consolidated GR/K3B specimens were instrumented in the 0° fiber direction and the other three were instrumented in the 90° fiber direction.

Three specimens of aluminum alloy (Al 2219-T87) and three titanium alloy (Ti) specimens were also instrumented and tested. All of these specimens were 2-in. by 2-in. square specimens with a tolerance of approximately ±0.125 inches.

Three aluminum-lithium alloy (Al-Li 2195-T87) specimens were tested. They were only 1-in. by 2-in. with the gages measuring strain in the rolled direction (see Figure 6). Although Al-Li is an anisotropic material, the load is introduced in the rolled direction in planned uniaxial tests, so measurements of strain gage thermal output were made in this direction only.

The 2-in. by 2-in. specimen size was picked to avoid "end effects" in the strain measurements, and since the gages measured strain in the rolled direction, the 1-in. by 2-in. Al-Li specimens were sufficient for measurement of thermal output data.

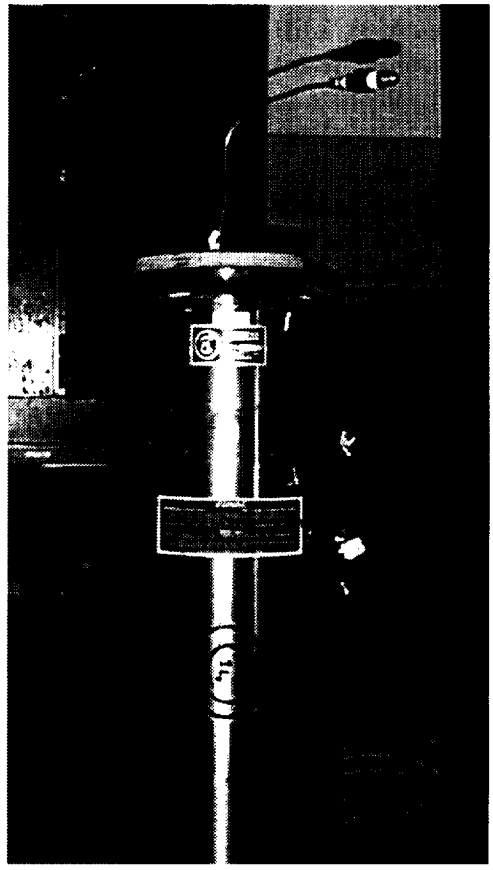

Figure 7. Dewar used for tests with spraybar and lid attached.

Experimental Apparatus

Due to the extreme temperatures required for this experiment, two different test apparatii were required. To obtain temperatures below -300°F, an insulated Dewar was used (see Figure 7). Specimens were placed in a wire basket (see Figure 8) and the basket was placed inside the Dewar. A spraybar was then inserted above the wire basket that allowed either liquid nitrogen or liquid helium to be admitted to the Dewar. This device setup allowed the measurement of strain readings at -450°F (liquid helium temperature) as well as -320°F (liquid nitrogen temperature).

In order to obtain test temperatures ranging from -300°F to 230°F, a large, insulated, forced convection chamber was used. This chamber, shown in Figure 9, was heated with resistive elements and cooled with a circulating liquid nitrogen sprayed "mist". The circulation of the liquid nitrogen mist helped assure uniform thermal conditions and prevented the liquid from directly contacting the specimens. All of the specimens were placed on a wire tray suspended approximately 2 in. above the bottom of the chamber to insure proper circulation around the specimens for temperature uniformity. Access ports and gaps on the top and bottom of the forced convection chamber were sealed to minimize leakage.

For data acquisition, a Neff data acquisition system (DAS) and the Autonet data acquisition software were used; both of which are available commercially. A photograph of the system is shown in Figure 10.

The Neff DAS utilized Wheatstone bridge [6] cards to measure strain (balanced to zero the strain gage readings at room temperature), and thermocouple cards to measure temperature. The signals were received, processed, and displayed on a computer using the Autonet software package.

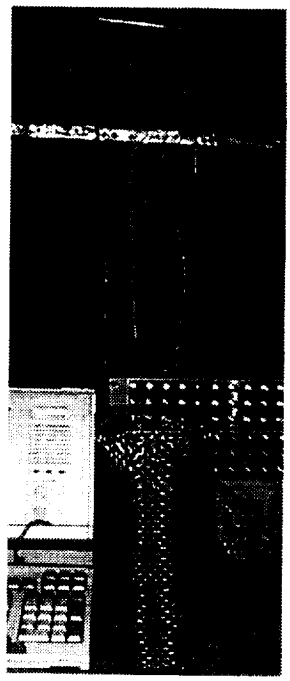

Figure 8. Wire basket used for Dewar tests.

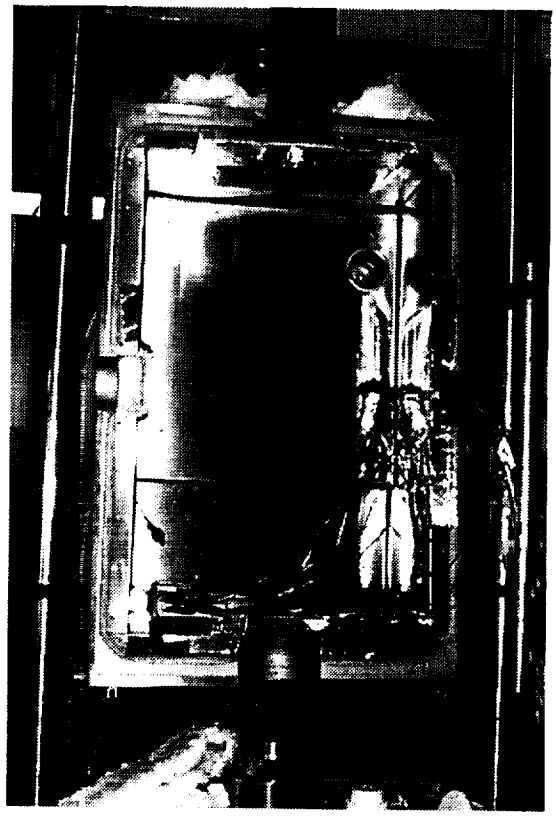

Figure 9. Convection chamber with specimens on tray.

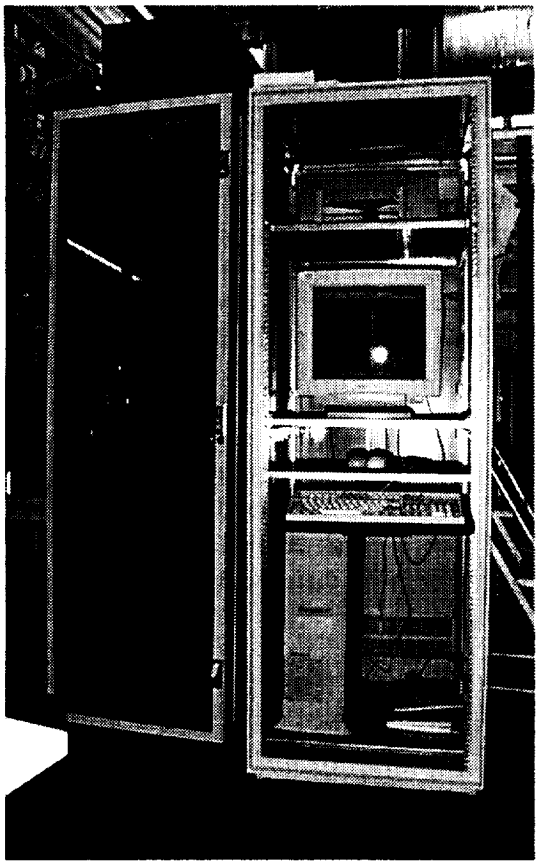

Figure 10. Neff/Autonet data acquisition system.

Although the Type-T thermocouples attached to the samples could be used to measure temperatures down to -450°F, the Autonet data conversion tables were only programmed for temperatures down to approximately -340°F, and when temperatures dropped below this value, the values were marked "out-of-range". For this reason, two actions were taken: first, a millivolt reading was taken from the thermocouples for later data reduction and second, Type-E thermocouples, capable of being processed by Autonet to temperatures of -450°F, were used to evaluate the temperature inside both the Dewar and the convection chamber. In the forced convection chamber, these Type-E thermocouples were placed in a diagonal pattern across the tray that held the specimens. For the Dewar tests, the specimen basket was lined with three Type-E thermocouples in a spiraling fashion with one at the top, one in the middle, and one on the bottom. These steps were taken to assess the temperatures and temperature variations very near the specimens as well as to provide a temperature measurement for temperatures below -340°F.

Experimental Procedure

Prior to a test, the strain gages and thermocouples were connected to the DAS. The strain gages were zeroed at room temperature by balancing the Wheatstone bridges in the DAS with a tolerance of ±5 microstrain. The thermocouple readings were then checked for proper function. The reference temperature at which the gages are zeroed is 70°F (room temperature).

Chamber Tests

The specimens were placed on a wire tray in the test chamber and the instrumentation wires were taped to the tray to keep the specimens stationary during the test (see Figure 11).

After the specimens were placed on the tray, three Type-E thermocouples were positioned on the wire tray with the thermocouple junctures placed as close to the specimens as possible in order to get an accurate reading of the ambient temperature in the chamber at the level of the specimens.

Figure 11. Specimens on platform within chamber.

Aluminum tape and Cryolite™ insulation were used to seal the perimeter of the closed chamber (located at the juncture of the two doors), the bundle of instrumentation wires exiting the test chamber, and the access ports of the chamber.

The first step in the testing procedure was to cool down the specimens to cryogenic temperature. In this chamber -300°F was the desired minimum temperature, but due to a degraded blower motor, it proved very difficult to hold this test temperature consistently so the minimum test temperature was raised to -270°F. Once the measured temperatures reached the desired test temperature of -270°F, the specimens soaked at temperature allowing them to reach a steady-state condition (approximately 5 min.). A variance of up to 5°F was allowed due to the temperature control limitations of the forced convection chamber. Data was logged on the computer for this 5-min. interval at a rate of 1 scan per second to insure minimal fluctuation and a steady state condition. After the 5-min. hold, the data for the particular test temperature were recorded in the logbook for each specimen. Data were taken at increments of 50°F with readings taken for test temperatures between -270°F and 220°F. After obtaining data at all the test temperatures, the specimens and gages were allowed to return to room temperature, were inspected for damage. The test was repeated two more times, and then the specimens and gages were again inspected for damage and repaired if necessary. After this final inspection, the specimens were removed and prepared for the Dewar tests.

Dewar Tests

The next portion of the test involved placing the specimens in a Dewar that was then cooled with either liquid nitrogen or liquid helium. The specimens were removed from the convection chamber and separated according to material type. It was determined that the complete specimen set could not fit into the Dewar, so the GR/EP specimens, the GR/BMI specimens, the aluminum-lithium specimens, and the aluminum alloy specimens were tested together. The remaining specimens (GR/K3B and Ti) were tested separately.

The specimens were placed in the wire basket shown in Figure 8 and inspected to insure they could hang freely in the wire basket while making minimal contact with one another. The basket was then prepared for the test by placing the three Type-E thermocouples in the basket, and then the basket was lowered into the Dewar. The spraybar was then placed inside the Dewar approximately 2 ft. above the specimens, and the lid was loosely placed on top of the Dewar. This was done to avoid spraybar contact with the specimens and to allow venting from the Dewar due to the vaporization of the cryogen. The nitrogen or helium supply was then attached to the port on the spraybar.

As with the tests in the chamber, the specimens were cooled to the test temperature and allowed to soak at that temperature for 5 min. as data was logged by the computer. After 5 min. a strain reading was recorded in the logbook. The liquid nitrogen flow into the Dewar was manually controlled and a test temperature of -315°F was achieved. The measurement using liquid helium to cool the specimens followed the same procedure and test temperatures of -454°F were achieved. In order to obtain a statistically significant sample of the data, all tests were repeated two more times.

Experimental Results and Analysis

The reduction of the data from this experiment required an average of the thermal output for each material type at each test temperature. For example, nine data values for thermal output, obtained for the three 0° GR/EP specimens at a given temperature from three separate tests were averaged to produce one value of thermal output for that material and material direction. A 95% confidence interval was calculated for each test material at each test temperature using the procedure outlined in Reference [7]. These intervals ranged from ±0.5 microstrain (±1%) for the AL-LI specimen at 230°F to ±321.1

microstrain (±10%) for the GR/K3B cured laminate at -421°F, indicating little scatter in the data. Once the data were obtained for all desired temperatures and averaged, a plot of the thermal output vs. temperature was generated. A commercial spreadsheet package was used to fit a fourth-order polynomial to the data points, generating an equation for that curve. A least squares fit through the data is used to calculate this curve. A fourth order polynomial was used because the manufacturer provides a fourth order polynomial and it accurately captures the variations in the data.

An initial comparison was made between the experimental values of thermal output and those values produced by the gage manufacturer. The manufacturer's data were obtained from gages mounted to a titanium silicate reference material. Because the reference material has a different coefficient of thermal expansion than the materials tested, the values of thermal output must be corrected for differences in coefficients of thermal expansion. Equation (3) illustrates the equation suggested by the manufacturer [3] to correct the thermal output:

$$e_R = e_P + (\alpha - \alpha_R)\Delta T \qquad (3)$$

Figure 12 contains both the experimentally determined thermal output and the corrected manufacturer's data for the titanium alloy (Ti). In this and subsequent plots of thermal output, the gage factor is not corrected for temperature. As shown in the Figure, the manufacturer's thermal output curve (corrected using Eq. (3)) does not closely approximate the experimental data (differing by a maximum of -408 microstrain (34.3%) at -409°F). For other materials the corrected manufacturer's data were acceptable at temperatures above -200°F, but proved to be less than satisfactory at cryogenic temperatures. For this reason it is preferable to directly determine the thermal output of the gages on a test material or specimen. These data can then be subtracted from the test data to determine true mechanical strain using Eq. (2a) [4].

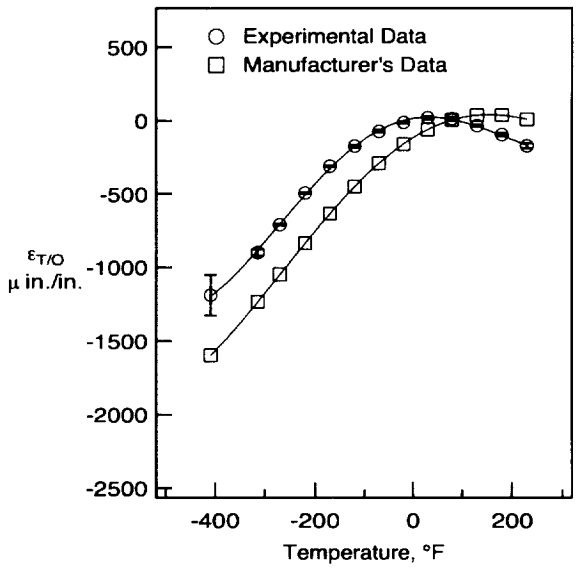

Figure 12. Thermal output for titanium (experimental data and strain gage manufacturer's data).

Figure 13 contains the thermal output data for the aluminum and aluminum-lithium alloys. The 95% confidence intervals are also shown for these and subsequent data as well as the fourth-order polynomials that were fitted to the data. The fourth order polynomial fitted to the data for this material and those for subsequent materials are given in Table 1.

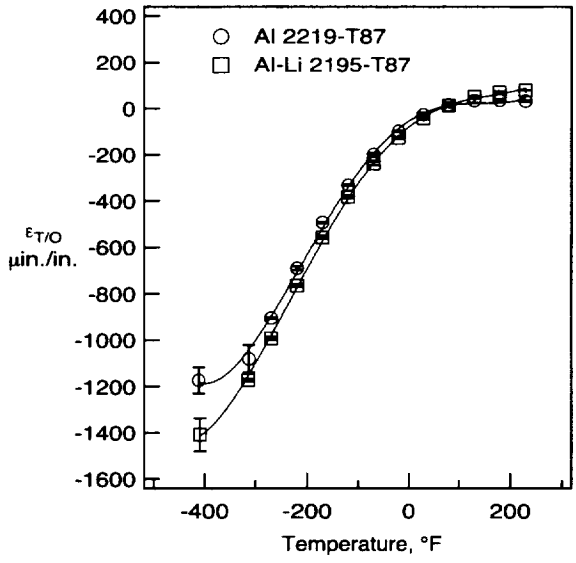

Figure 13. Thermal output data for Al and AL-LI with a gage factor of 2.08.

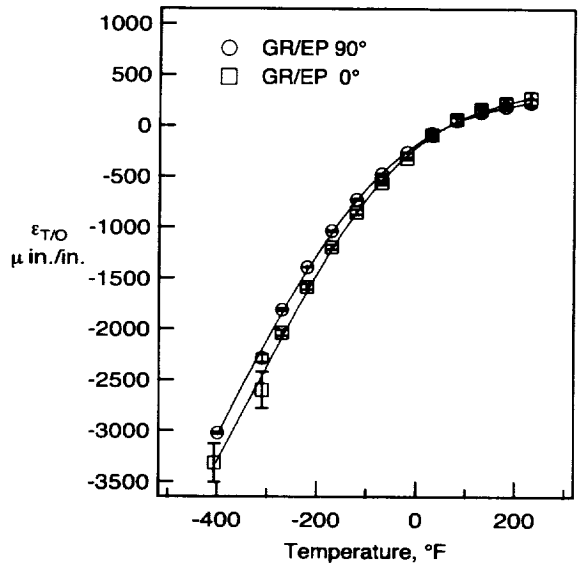

Figure 14. Thermal output data for GR/EP with a gage factor of 2.02.

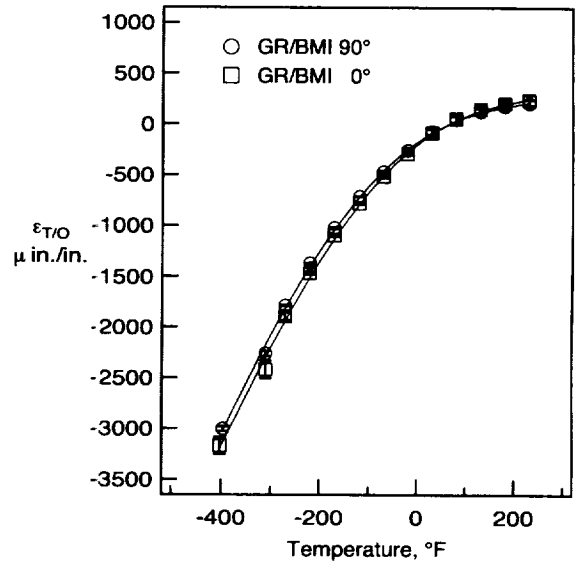

Figure 15. Thermal output for GR/BMI specimens with a gage factor of 2.02.

Figure 14 contains plots of the thermal output data for the graphite-epoxy (IM7/977-2) specimens with a $[\pm 45/0/90/0]_S$ ply lay-up. Data in both the 0° ply orientation direction and the 90° direction are given.

Figure 15 contains plots of the thermal output data for the graphite-bismaleimide (IM7/5260) specimens with a $[\pm 45/0/90/0]_S$ ply lay-up. Data are given for both the 0° ply orientation direction and the 90° direction. Fourth-order polynomials for both ply orientation directions were generated.

Thermal output data for the graphite-thermoplastic (GR/K3B) specimens are given in Figure 16. Thermal output data for both the specimens extracted from the facesheets of a co-cured sandwich structure and those fabricated from a cured laminate are given in both the 0° and 90° ply orientation direction.

Figure 17 contains the thermal output data in the 0° ply direction for all of the materials tested. The thermal output data for gages mounted on metals differ greatly from those mounted on composite materials, but variations among the metals and composite materials were relatively low.

For the metals, the largest variation in thermal output occurs at -273°F and is 281 microstrain. For the composite materials in the 0° ply direction, the maximum variation is 399 microstrain and occurs at -423°F.

The 95% confidence intervals calculated for the thermal output data gathered during the chamber tests are relatively small and indicate a

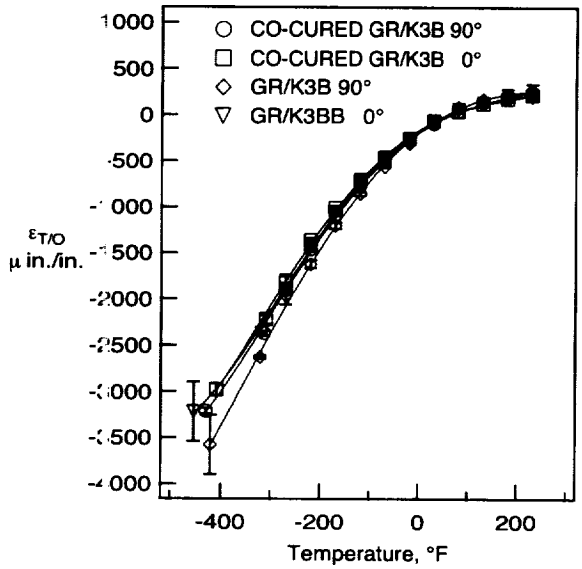

Figure 16. Thermal output data for GR/K3B with a gage factor of 2.02.

minimum of scatter in the data for all the materials at test temperatures above -270°F. For the thermal output data gathered during the Dewar tests, the 95% confidence intervals calculated indicate a large scatter in the data at temperatures below -270°F for all the materials tested. This is primarily due to the wider test temperature variations observed in the Dewar test.

All the data collected are summarized in Table 1. Listed are the fourth order polynomial equations determined for each material, the minimum and maximum temperature to which each material was subjected, and the minimum and maximum measured thermal output. The maximum error between the manufacturer's provided thermal output, corrected by equation (3), and the experimental thermal output is also given. Note that this difference is the absolute strain error that would result if the manufacturer's thermal output data were used to correct for thermal output, rather than the experimentally determined thermal output data.

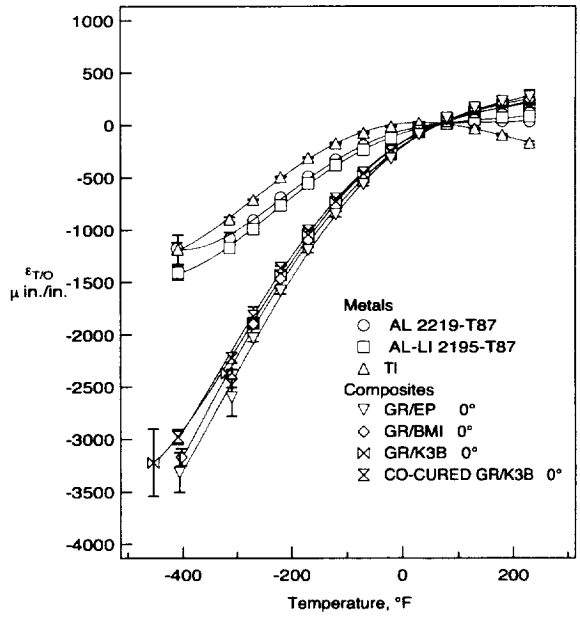

Figure 17. Thermal output data in the 0° fiber direction for all materials tested.

Table 1. Summary of Thermal Output Data.

Material	Temperature, °F		Strain, μstrain		Fourth Order Model of Thermal Output, $e_{T/O}$, μstrain	Max |Δ Error|,
	Min.	*Max.*	*Min.*	*Max.*		μstrain (%)
Composites						
GR/EP 0^0	-400	230	-3316	291	$-211.42 + 3.9755T - 0.0112T^2 + 7x10^{-6}T^3 + 3x10^{-8}T^4$	1731 (52)
GR/EP 90^0	-406	230	-3023	241	$-181.16 + 3.3991T - 0.0096T^2 + 7x10^{-6}T^3 + 2x10^{-8}T^4$	1461 (48)
GR/BMI 0^0	-403	230	-3169	263	$-200.55 + 3.6989T - 0.0099T^2 + 6x10^{-6}T^3 + 2x10^{-8}T^4$	1593 (48)
GR/BMI 90^0	-397	230	-3001	227	$-177.80 + 3.3392T - 0.0095T^2 + 7x10^{-6}T^3 + 2x10^{-8}T^4$	1446 (50)
Co-Cured GR/K3B 0^0	-409	230	-2976	228	$-167.67 + 3.2353T - 0.0103T^2 + 9x10^{-6}T^3 + 3x10^{-8}T^4$	1381 (46)
Co-Cured GR/K3B 90^0	-430	230	-3210	260	$-191.43 + 3.5523T - 0.0105T^2 + 8x10^{-6}T^3 + 3x10^{-8}T^4$	1549 (43)
GR/K3B 0^0	-454	230	-3220	201	$-165.95 + 3.4110T - 0.0113T^2 + 8x10^{-6}T^3 + 4x10^{-8}T^4$	1494 (46)
GR/K3B 90^0	-421	230	-3577	253	$-192.23 + 4.1037T - 0.0111T^2 + 3x10^{-6}T^3 + 2x10^{-8}T^4$	1943 (54)
Metals						
Al-Li 2195-T87	-411	230	-1408	80	$-81.26 + 1.7143T - 0.0069T^2 + 5x10^{-6}T^3 + 3x10^{-8}T^4$	254 (43)
AL 2219-T87	-411	230	-1173	38	$-55.31 + 1.4220T - 0.0077T^2 + 6x10^{-6}T^3 + 4x10^{-8}T^4$	504 (18)
Titanium	-409	230	-1188	23	$12.57 + 0.5643T - 0.0084T^2 + 5x10^{-6}T^3 + 3x10^{-8}T^4$	408 (34)

Concluding Remarks

From the data gathered and the plots produced, one can conclude that the testing procedure produced very repeatable experimental results. Strain gage manufacturers produce plots and equations for thermal output as a function of temperature and also provide gage factor variations with temperature for gages mounted to a wide variety of standard materials. However, the manufacturer's methodology to correct for nonstandard materials was found to be inaccurate, especially at cryogenic temperatures. For the materials, lay-ups and temperatures of concern, the absolute errors associated with using the thermal output data provided by the strain gage manufacturer are too high and so experimentally determined thermal output data must be used. The maximum variation in thermal output among the composite materials is moderate, and if data for a different material system is lacking, any of the composite data presented here could be used as a first approximation to the thermal output.

References

1. Cook, Stephen A., "The X-33 Advanced Technology Demonstrator", AIAA-96-1195, Presented at the AIAA Dynamics Specialists Conference, April 18-19, 1996.

2. Johnson, Theodore F., R. Natividad, H. K. Rivers, R. Smith, "Thermal Structures Technology Development for Reusable Launch Vehicle Cryogenic Propellant Tanks", Presented at the Third Space Technology and Application International Forum Conference on Next Generation Launch Vehicles, January 25-29, 1998.

3. Anonymous, "Strain Gage Thermal Output and Gage Factor Variation with Temperature", Micromeasurements Group-TN-504-1, 1993.

4. Anonymous, "Temperature-Induced Apparent Strain and Gage Factor Variation in Strain Gages", Micromeasurements Group-TN-504, 1983.

5. Moore, Thomas C., "Recommended Strain Gage Application Procedures for Various Langley Research Center Balances and Test Articles", NASA TM-110327, March 1997.

6. Dally, James W., and W. F. Riley, *Experimental Stress Analysis*, Third ed., McGraw-Hill, Inc., 1991.

7. Coleman, Hugh W., W. Glenn Steele, *Experimentation and Uncertainty Analysis*, pp 17-37, J. Wiley & Sons, 1989.

REPORT DOCUMENTATION PAGE

Form Approved
OMB No. 0704-0188

1. AGENCY USE ONLY (*Leave blank*)	2. REPORT DATE	3. REPORT TYPE AND DATES COVERED
	October 1998	Technical Memorandum

4. TITLE AND SUBTITLE
Thermal Output of WK-Type Strain Gauges on Various Materials at Cryogenic and Elevated Temperatures

5. FUNDING NUMBERS
242-33-01-08

6. AUTHOR(S)
Matthew K. Kowalkowski, H. Kevin Rivers and Russell W. Smith

7. PERFORMING ORGANIZATION NAME(S) AND ADDRESS(ES)
NASA Langley Research Center
Hampton, VA 23681-2199

8. PERFORMING ORGANIZATION REPORT NUMBER
L-17752

9. SPONSORING/MONITORING AGENCY NAME(S) AND ADDRESS(ES)
National Aeronautics and Space Administration
Washington, DC 20546-0001

10. SPONSORING/MONITORING AGENCY REPORT NUMBER
NASA/TM-1998-208739

11. SUPPLEMENTARY NOTES

12a. DISTRIBUTION/AVAILABILITY STATEMENT
Unclassified-Unlimited
Subject Category 15 Distribution: Nonstandard
Availability: NASA CASI (301) 621-0390

12b. DISTRIBUTION CODE

13. ABSTRACT (*Maximum 200 words*)
Strain gage apparent strain (thermal output) is one of the largest sources of error associated with the measurement of strain when temperatures and mechanical loads are varied. In this paper, experimentally determined apparent strains of WK-type strain gages, installed on both metallic and composite-laminate materials of various lay-ups and resin systems for temperatures ranging from -450°F to 230°F are presented. For the composite materials apparent strain in both the 0° ply orientation angle and the 90° ply orientation angle were measured. Metal specimens tested included: aluminum-lithium alloy (Al-LI 2195-T87), aluminum alloy (AL 2219-T87), and titanium alloy. Composite materials tested include: graphite-toughened-epoxy (IM7/997-2), graphite-bismaleimide (IM7/5260), and graphite-K3 (IM7/K3B). The experimentally determined apparent strain data are curve fit with a fourth-order polynomial for each of the materials studied. The apparent strain data and the polynomials that are fit to the data are compared with those produced by the strain gage manufacturer, and the results and comparisons are presented. Unacceptably high errrors between the manufacture's data and the experimentally determined data were observed (especially at temperatures below -270°F).

14. SUBJECT TERMS
Apparent Strain, Thermal Output, Cryogenic, Temperature, Composite, Aluminum Aluminum-Lithium, Titanium

15. NUMBER OF PAGES
17

16. PRICE CODE
A03

17. SECURITY CLASSIFICATION OF REPORT	18. SECURITY CLASSIFICATION OF THIS PAGE	19. SECURITY CLASSIFICATION OF ABSTRACT	20. LIMITATION OF ABSTRACT
Unclassified	Unclassified	Unclassified	